Journal of Petrology, 2026, **67**(7), egag052
https://doi.org/10.1093/petrology/egag052
Published: 17 JUNE 2026
Letter

OXFORD

Dehydration of Metasedimentary Rocks Triggers Early Water-Flux Melting of Metagranitoids and Influences Strain Localization

JONAS VANARDOIS* and PIERRE LANARI

Institute of Earth Sciences, University of Lausanne, Géopolis, Lausanne CH-1015

*Corresponding author: Telephone: +33(0) 606 755 562; E-mail: jonas.vanardois@unil.ch
Handling Editor: Prof. Joerg Hermann

Large melt volumes in metagranitoid lithologies are described in numerous orogens and often play a major role in the strain distribution within the orogenic crust. In a continental crust devoid of free water, melt fractions above 10 vol % in metagranitoid rocks can only be generated by the influx of external water via a fluid phase. One possible origin of these aqueous fluids is the subsolidus dehydration of the surrounding metasedimentary rocks. To test this hypothesis, a path-dependent multi-system phase equilibrium model was developed. This model simulates the amount of aqueous fluid produced by a metasedimentary system in the temperature interval between the solidus of the orthogneiss and that of the metasediment. This amount of aqueous fluid is transferred to the orthogneiss system, and the new melt fraction is calculated. This simulation was carried out along eight prograde Pressure–Temperature (*P*–*T*) paths using metapelite/orthogneiss and metagraywacke/orthogneiss associations. The results show that metasedimentary rocks produce between 0.01 and 0.2 wt % of aqueous fluid due to the breakdown of staurolite and paragonite, and the minor consumption of muscovite and biotite. Nevertheless, the small amount of aqueous fluid increases the melt fractions of the orthogneiss system by several percent, making orthogneiss the most fertile lithology along most prograde paths at temperatures below 750°C and pressures from 0.5 to 1.5 GPa. If less than half of the crust is composed of orthogneiss, the volume of melt generated in the orthogneiss is sufficient to significantly weaken it, allowing deformation to localize within the orthogneiss bodies. We propose that this strain localization situation creates preferential pathways for additional fluid influxes, which enhances partial melting in metagranitoid lithologies and creates a positive feedback loop. Our results suggest that this process may occur in most prograde *P*–*T* paths in orogenic crusts composed of metasedimentary rocks and orthogneisses.

Keywords partial melting, aqueous fluid influx, heterogeneous orogenic crust, path-dependent thermodynamic modeling

Introduction

Experimental studies have shown that a small percentage of melt is enough to significantly decrease the differential strength necessary to deform rocks (Rosenberg & Handy, 2005). This has a major control on strain localization within the orogenic crust (Mancktelow, 2002; Gardner *et al.,* 2017; Piazolo *et al.,* 2020). Thus, strain localization and orogenic evolution in the middle and lower orogenic crust are mainly controlled by the occurrence of partial melting (Vanderhaeghe, 2009). Metapelite is typically considered the most fertile lithology in the crust because it can produce large quantities of melt through micas dehydration reactions (Clemens & Vielzeuf, 1987; Clemens, 2012; Brown, 2013; Clemens *et al.,* 2020) and likely play a major role on strain localization. Due to the absence of aqueous fluid in the middle and lower orogenic crust, water-flux reactions are assumed to have a limited contribution to melt production (Thompson, 1983; Yardley, 2009, 2012; Tafur & Diener, 2020). However, several studies have documented large melt fractions (> 10 vol %) in metagranitoid lithologies resulting from water-flux melting (White *et al.,* 2005; Sawyer, 2010; Weinberg & Hasalová, 2015) and discussed their role on strain localization during orogenic evolution (Vanardois *et al.,* 2024; Tao *et al.,* 2025; Fig. 1). However, these reactions require the addition of external aqueous fluid to generate melt quantities higher than 5–10 vol % (Gardien *et al.,* 2000; Hasalová *et al.,* 2008; Webb *et al.,* 2015).

Aqueous fluid influx can be generated by a mantle source (e.g. Collins *et al.,* 2020; Volante *et al.,* 2025), the crystallization of hydrous magmas (e.g. Annen & Sparks, 2002; Davidson *et al.,* 2007; Villaros *et al.,* 2018; Couzinié *et al.,* 2021), or by subsolidus metamorphic dehydration reactions in H_2O-rich lithologies (metapelites) during prograde metamorphism (e.g. White *et al.,* 2005; Berger *et al.,* 2008; Sawyer, 2010). The hypotheses invoking external sources, such as the mantle and magmas, require pathways in the orogenic crust through which aqueous fluid or melt could migrate efficiently (Weinberg & Hasalová, 2015; Tafur & Diener, 2020). In contrast, studies have proposed that the presence of aqueous fluid during partial melting of orthogneiss can trigger the formation of crustal-scale shear zones (e.g. Vanardois *et al.,* 2024; Tao *et al.,* 2025). These results suggest the presence of an in-situ or nearby source of aqueous fluid during the partial melting of the orthogneisses. It has been proposed that aqueous fluid generated by the dehydration of metasedimentary rocks

RECEIVED JANUARY 22, 2026. **REVISED** JUNE 9, 2026. **ACCEPTED** JUNE 12, 2026

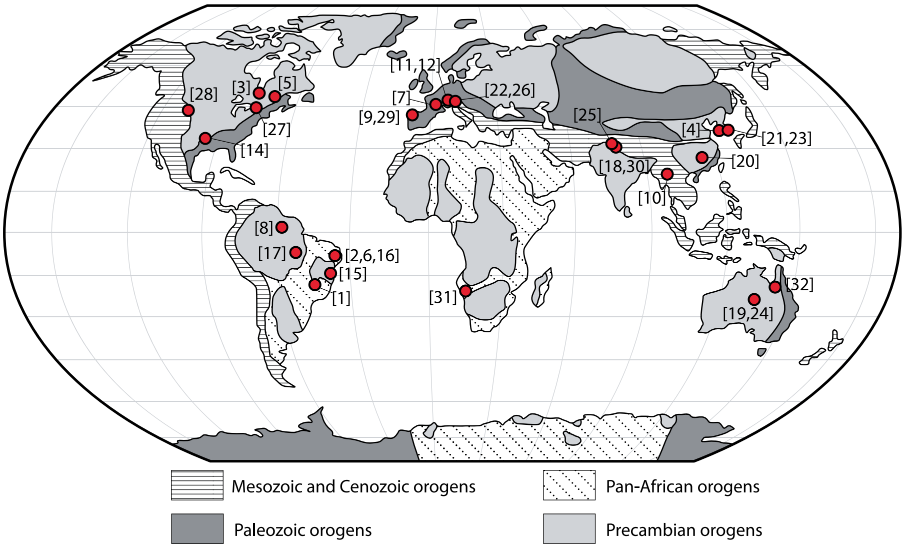

Figure 1 Overview of studies documenting strain localization related to water-flux partial melting of metagranitoid lithologies. The base map is modified from Liou *et al.* (2004). [1] Carvalho *et al.*, 2016; [2] França *et al.*, 2019; [3] Sawyer, 2010; [4] Lee & Cho, 2013; [5] Lambert *et al.*, 2023; [6] Viegas *et al.*, 2014; [7] Couzinié *et al.*, 2021; [8] Scalabrin *et al.*, 2025; [9] García-Arias *et al.*, 2015; [10] Tao *et al.*, 2025; [11] Vanardois *et al.*, 2022; [12] Vanardois *et al.*, 2024; [13] Levy *et al.*, 2025; [14] Levine, 2011; [15] Sperandio *et al.*, 2025; [16] Ferreira *et al.*, 2021; [17] Delinardo-Silva *et al.*, 2025; [18] Kumar *et al.*, 2022; [19] Varga *et al.*, 2022; [20] Li *et al.*, 2023; [21] Lee *et al.*, 2023; [22] Mintrone *et al.*, 2022; [23] Lee & Cho, 2020; [24] Collins *et al.*, 1989; [25] Pognante, 1992; [26] Burri *et al.*, 2005; [27] Slagstad *et al.*, 2005; [28] Mogk, 1992; [29] Escuder Viruete, 1999; [30] Reichardt *et al.*, 2010; [31] Jung *et al.*, 2009; [32] Volante *et al.*, 2020.

surrounding metagranitoid lithologies can be the in-situ or nearby source of free water (e.g. White *et al.*, 2005; Droop & Brodie, 2012). Indeed, metagranitoid rocks start melting at lower temperatures than metasedimentary rocks because the presence of Kfs allows the wet-solidus granite melting reaction (Kfs + Pl + Qz + H_2O (+ Ms) → L; Johannes & Holtz, 1996; mineral abbreviations are from Warr (2021), L is for liquid) to occur. Metasedimentary rocks generally lack Kfs in the Ms stability field above 0.3 GPa and start melting with the breakdown of Pl (Pl + Ms + Qz + H_2O → L; Patiño Douce & Harris, 1998). This difference creates a *P*–*T* window between the two solidi in which the metagranitoid lithologies are partially molten, while the metasedimentary lithologies remain free of melt (Fig. 2a). Water-flux partial melting induces a decrease in the total volume of the system, thereby draining surrounding fluids (Clemens & Droop, 1998; Mancktelow, 2006). Therefore, one can assume that aqueous fluid produced by unmolten metasedimentary lithologies will flow into partially molten metagranitoid rocks, increasing their melt production (Clemens & Droop, 1998; Fig. 2a). This study aims to determine whether the amount of aqueous fluid produced by metasedimentary lithologies in the *P*–*T* window between the two solidi can increase the melt fraction within the metagranitoid lithologies enough to control strain localization. A path-dependent multi-system thermodynamic model has been developed to simulate this process and quantify the melt fractions along several prograde *P*–*T* trajectories.

Methodology

A program allowing path dependent phase equilibrium modeling of a multi-lithological system was developed using the Julia programming language (Fig. 2b; WaterMeltPT.jl). The three most abundant lithologies in the orogenic crust—metapelite, metagraywacke and orthogneiss—were considered. The bulk rock compositions were taken from Forshaw & Pattison (2023) for the metapelite, Weisbrod (1970) for the orthogneiss and Vielzeuf & Montel (1994) for the metagraywacke (Table S1). In each simulation, a mixed system (metapelite + orthogneiss or metagraywacke + orthogneiss) follow the same *P*–*T* trajectory. After each *P*–*T* increment, the stable phase assemblage is calculated using Gibbs free energy minimization and the MAGEMin_C software (Riel *et al.*, 2022). The solution models of White *et al.* (2014) were used in the NCKFMASHT system. The *P*–*T* increment was set to 1°C to reflect efficient re-equilibration and absence of overstepping (Markmann & Lanari, 2026) and slopes are +3 MPa/°C, +0 MPa/°C or − 3 MPa/°C as a function of the trajectory (increasing *P*, isobaric or decreasing *P*, respectively).

When all lithologies are below subsolidus conditions, aqueous fluid generated at T_n–P_n is extracted from both systems, and no fraction is kept in a fluid-filled porosity (Fig. 2). When the orthogneiss system reaches the wet solidus at T_n–P_n, the aqueous fluid generated *in-situ* at T_n–P_n is immediately consumed by water-flux melting reactions by the orthogneiss. In addition, the fraction of aqueous fluid produced by the unmolten metasedimentary system predicted by the first Gibbs free energy minimization is transferred to the partially molten orthogneiss system before performing the second free Gibbs energy minimization. When partial melting begins in the metasedimentary system, an aqueous fluid is no longer present and fluid exchanges cease. From this point on, both systems evolve as closed systems. In our model, aqueous fluids are composed exclusively of water (pure H_2O). Because temperature conditions tested remain below 750°C, garnet growing during the prograde path is kept metastable and its composition is thus removed from the reactive bulk composition for the rest of the *P*–*T* path. Therefore, the model fractionates garnet from the reactive system volume along the prograde trajectories. Bulk compositions are renormalized at each step by MAGEMin_C. Melt extraction was not considered because the predicted melt fractions remain mainly below the threshold considered as the limit for melt extraction (i.e. 7 vol % of melt; Rosenberg & Handy, 2005). Additionally, the total volume

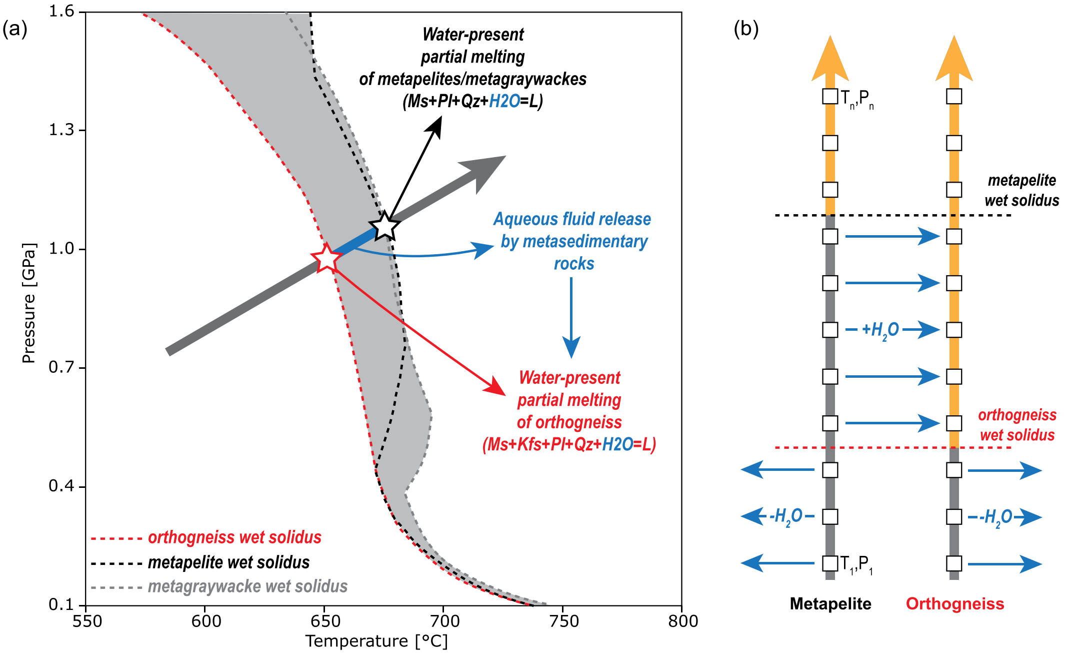

Figure 2 (a) *P–T* diagram showing the wet solidus for orthogneiss, metapelite and metagraywacke, as well as the *P–T* window (in gray) between the solidi in which the orthogneiss is partially molten and metasedimentary rocks are not. The arrow represents an arbitrary prograde path that passes through this P–T window. Under these conditions, metasedimentary rocks can release aqueous fluid. If this water is transferred to the orthogneiss, it can trigger water-flux partial melting. (b) Schematic representation of the path-dependent multi-lithology model along the arbitrary P–T trajectory. The blue arrows indicate aqueous fluid extraction from the systems (-H_2O) or water exchange between the two systems (+H_2O).

decrease induced by water-flux melting reactions can also prevent melt extraction (Clemens & Droop, 1998; Etheridge *et al.,* 2021).

For each step, the predicted phase modes (in molar quantity) are saved and shown as mode box diagrams to illustrate the metamorphic evolution of each system (Fig. 3a and b). The amount of aqueous fluid produced by the metasedimentary system and transferred to the orthogneiss system is the aqueous fluid molar fraction difference between the solidus temperatures of the two lithologies used during the calculation (Fig. 3c and d). The molar melt fractions are calculated in the metasedimentary and in the orthogneiss systems with and without fluid transfer. To compare our results with experimental data, molar melt fractions were converted into volumetric melt fractions (Fig. 3e and f). The impact of the relative abundance between orthogneiss and metasedimentary rocks was investigated with 1/2 and 1/4 molar fractions (i.e. half of the crust is orthogneiss, and a quarter of the crust is orthogneiss). For instance, a crust composed of 1/4 molar fractions of orthogneiss, and 3/4 metasedimentary rock, the orthogneiss will receive three times more water than if the crust was composed of 1/2 orthogneiss and 1/2 metapelite.

Eight prograde *P–T* trajectories have been investigated, each of them from 600 to 750°C with various pressure gradients from positive to negative (Fig. 4) to represent the diversity of metamorphic evolutions occurring in the orogenic crust. Detailed results of all trajectories are available in supplementary data.

Results

Solidus conditions and melting reactions

For all eight simulated trajectories, the modeled solidus temperature of orthogneiss is consistently lower than that of metasedimentary rocks (Fig. 4a). The solidus of metagraywacke is predicted to occur at slightly higher temperatures (<20°C) than that of metapelites. The temperature difference increases with pressure (from 5 to 23°C; Fig. 4a). In orthogneiss, first melts are produced by the eutectic reactions $Kfs + Pl + Qz + H_2O \rightarrow L$ and $Ms + Kfs + Pl + Qz + H_2O \rightarrow L$. Because metasedimentary rocks are devoid of Kfs at these *P–T* conditions, their first melts are produced by the eutectic reaction $Ms + Pl + Qz + H_2O \rightarrow L$, occurring at slightly higher temperatures (~30–40°C; Patiño Douce & Harris, 1998; Weinberg & Hasalová, 2015). This difference of solidus temperature between lithologies is also observed in experimental data (Winkler & von Platen, 1958, 1960, 1961; Huang & Wyllie, 1973; Johannes & Holtz, 1996; Patiño Douce & Harris, 1998) and is induced by the hydrated breakdown of Kfs + Qz at lower temperatures than the hydrated breakdown of Pl + Qz (Patiño Douce & Harris, 1998). The anorthite content of plagioclase can have an impact on the solidus temperature conditions (Winkler & von Platen, 1961; Johannes, 1984) but is likely minor as plagioclase in orthogneiss are predicted to be more calcic than the ones in metasedimentary rocks (see supplementary files).

Amount of water

The amount of predicted free water produced during the prograde path depends on the destabilization of hydrous minerals into anhydrous or less hydrous ones. Reactions that produce a free aqueous fluid can be seen through mode box diagrams (Fig. 3a and b) and the aqueous fluid molar fraction along the trajectory (Fig. 3c and d). In the *P–T* window between the orthogneiss and the metasediment solidi, the main reactions that release aqueous fluid are related to the breakdown of staurolite ($St + Ms + Qz \rightarrow Ky + Pl + Bt + H_2O$) and paragonite ($Pg + Qz \rightarrow Ms + Pl + H_2O$), as well as a small consumption of Na-muscovite and biotite to produce anhydrous minerals such as

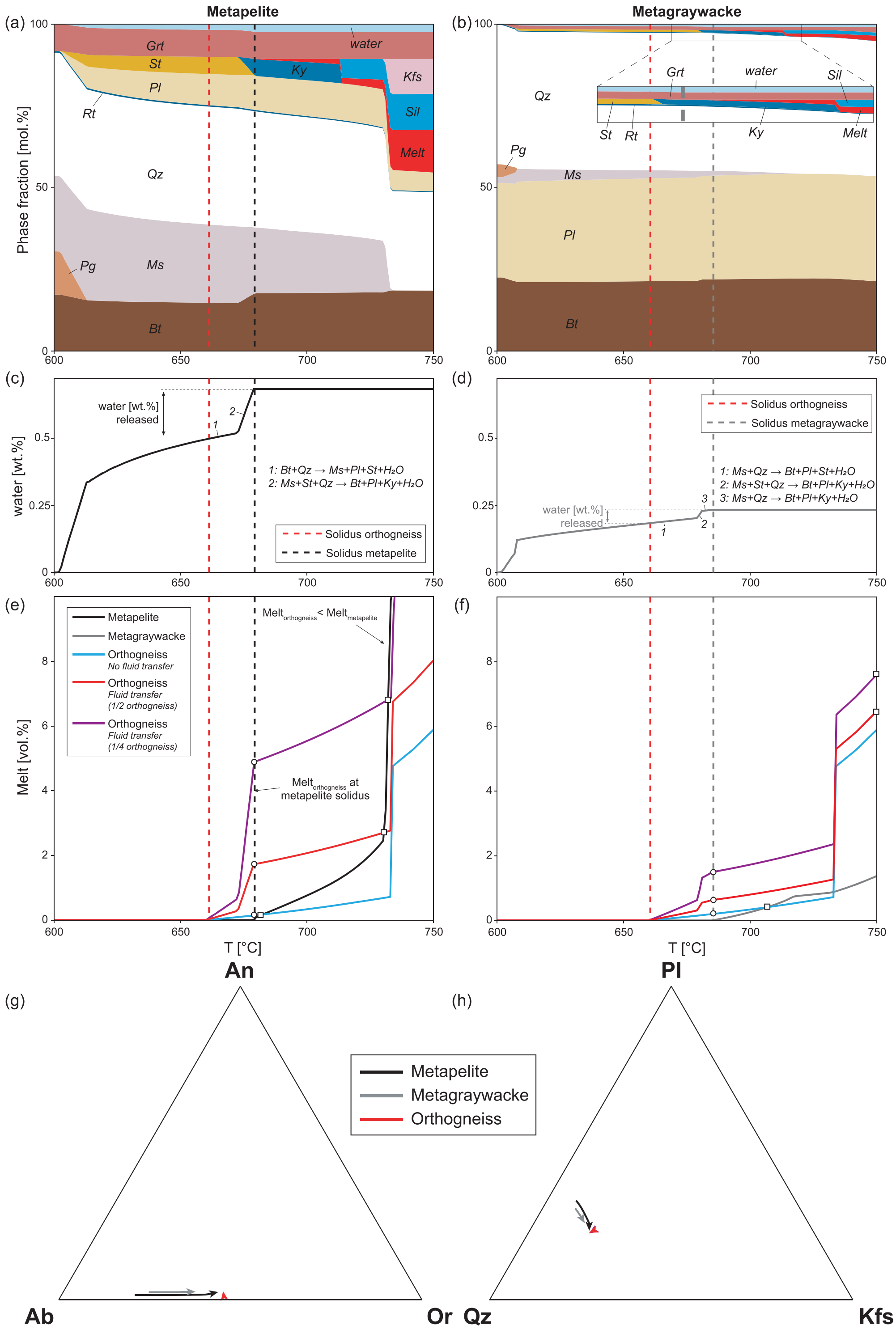

Figure 3 Results of the phase equilibrium simulation for trajectory 4 (isobaric, shown in Fig. 4). (a and b) Mode-box diagrams of the metasediment system for metapelite and metagraywacke. (c and d) Predicted water quantities (in wt %) released by the metasedimentary rocks within the P–T window between the two solidi. (e and f) Predicted melt fractions (in vol%) in orthogneiss and metasedimentary rocks as a function of the water exchange between the two systems and the molar fraction of orthogneiss. Circles represent the melt fractions in orthogneiss at the metasediment solidus (values in Fig. 4d and f). Squares represent the conditions at which metasedimentary rocks become more fertile than the orthogneiss (values and tips of arrows in Fig. 4c and e). (g and h) Albite–Anorthite–Orthoclase (Ab–An–Or) and Quartz–Plagioclase–K-feldspar (Qz–Pl–Kfs, Pl = An + Ab) ternary diagrams showing evolution of melt composition in function of temperature increase. Composition of melts in orthogneiss does not change if more water is added (cf. supplementary files).

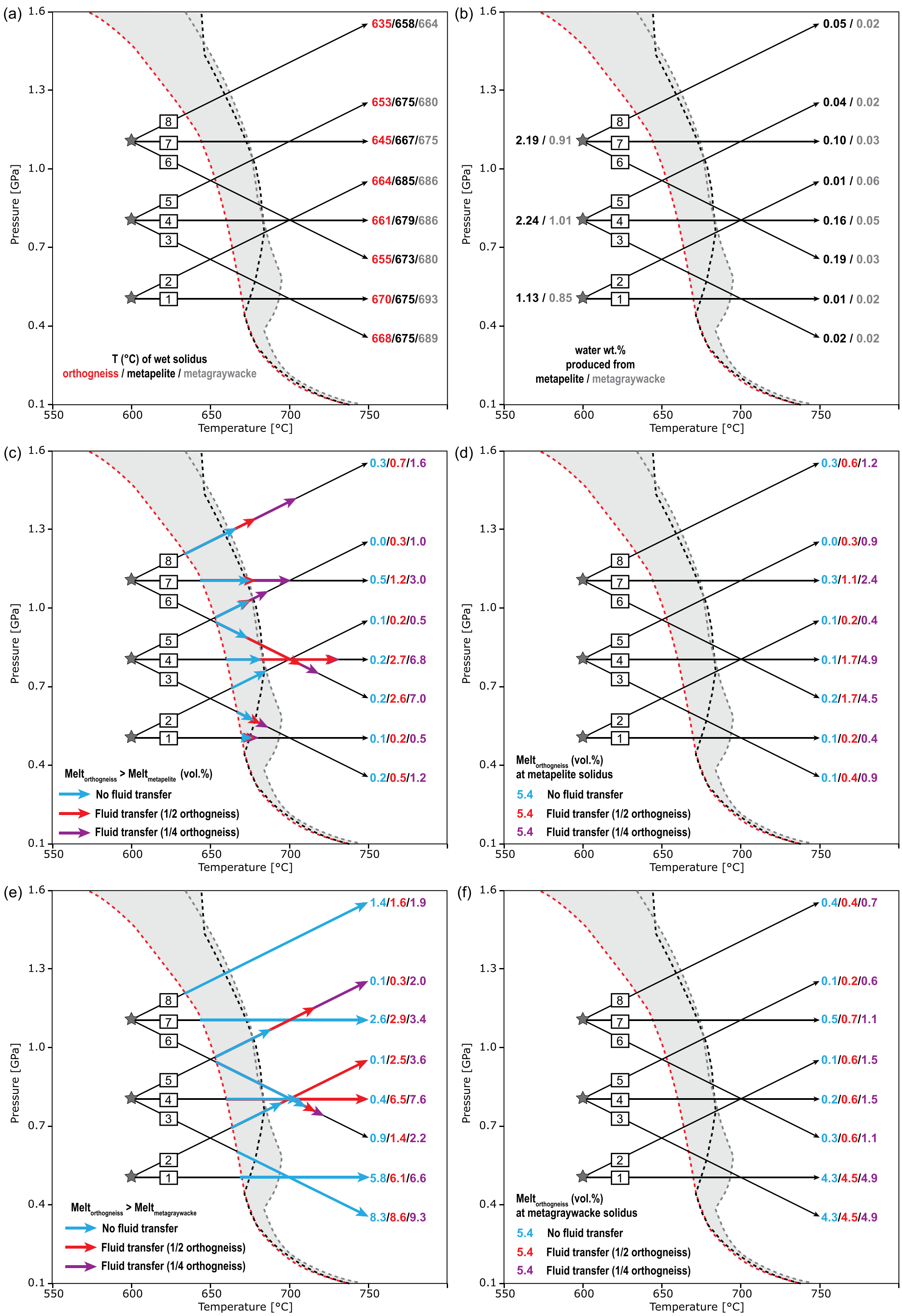

Figure 4 Results of the eight prograde *P*–*T* trajectories tested in this study. (a) Temperature conditions of the wet solidus for each lithology along the P–T trajectory. (b) Amount of aqueous fluid released (in wt %) by the metapelite (black) and by the metagraywacke (gray) between the two solidi (gray *P*–*T* window). Values at the left of trajectories indicate the initial amount of H_2O within these rocks (c and e) Arrows indicate the part of the trajectory where the orthogneiss is the most fertile lithology. The blue arrows represent the results without aqueous fluid exchange between the two systems. The red and purple arrows represent the results with water exchange and an orthogneiss fraction of ½ and ¼ of the system, respectively. The numbers represent the melt fractions in orthogneiss (in vol %) at the conditions where the metasedimentary rock (c: metapelite; e: metagraywacke) becomes more fertile (tips of the arrows). Where the tip of the arrow reaches 750°C, orthogneiss is the most fertile lithology, and numbers represent the melt fraction in orthogneiss at 750°C. (d and f) Melt fraction in orthogneiss (in vol %) at the metasedimentary rock solidus conditions (d: metapelite; f: metagraywacke) for calculations with and without water exchange.

plagioclase and garnet (e.g. Pg + Bt + Qz → Ms + Pl + Grt + H_2O; Na-Ms → Bt + Pl + Qz + H_2O).

The model results indicate that the metasedimentary rocks produce less than 0.2 wt % of aqueous fluid between their solidus and that of the orthogneiss (Fig. 4b). Since a metapelite contains more hydrous minerals than a metagraywacke, a greater amount of aqueous fluid is generally produced during the prograde path in metapelite than in metagraywacke (Fig. 4b).

Interestingly, the amount of aqueous fluid produced depends heavily on the *P*–*T* trajectory and not on their original H_2O contents (Fig. 4b). Trajectories starting from similar *P*–*T* conditions can yield very different results depending on their *P*–*T* slope. For example, trajectories 3, 4 and 5 all begin at 600°C and 0.8 GPa, with the same amount of aqueous fluid. However, the amount of aqueous fluid produced in the solidi window ranges from 0.02 to 0.16 wt % for the metapelite and from 0.02 to 0.05 wt % for the metagraywacke.

Melt production in orthogneiss

Two main results are used to discuss the significance of the melt production in orthogneiss compared to metasedimentary rocks for each *P*–*T* trajectory: (1) the temperature at which the metasedimentary rocks produced more melt than the orthogneiss, and the corresponding melt fraction in orthogneiss at these conditions (Fig. 4c and e) and (2) the amount of melt in the orthogneiss at the solidus conditions of the metasedimentary rocks (Fig. 4d and f).

The first observation is that the type of *P*–*T* trajectory strongly influences the produced melt fractions. Trajectories that start with similar *P*–*T* conditions generate different melt fractions. For instance, trajectories 6, 7, and 8 start at 600°C and 1.1 GPa and yield melt fractions of 7.0, 3.0 and 1.6 vol %, respectively, when associated with metapelites and a fraction of 1/4 orthogneiss (Fig. 4c). These results suggest that trajectories with isobaric or decreasing-*P* gradients can produce higher melt fraction in orthogneiss than trajectories with increasing-*P* gradients, but this effect is also dependent on the lithologies considered (e.g. trajectory 2 is inefficient with metapelite but important with metagraywacke) and on the metamorphic reactions encountered. The process is less efficient at lower *P* conditions because muscovite dehydration reaction occurs at lower temperature conditions. Results for the two metasedimentary rocks are discussed separately in the following section.

Metapelite & orthogneiss

Aqueous fluid exchange between the metapelite and orthogneiss increases the melt fraction produced by the orthogneiss and therefore the temperature at which the metapelite becomes the most fertile lithology (Fig. 4c). In particular, the *P*–*T* trajectories with higher amounts of aqueous fluid transferred from metasedimentary rocks (i.e. trajectories 4, 6, and 7) show an increase of melt fraction within the orthogneiss by several percent, up to +6.8 vol %, when orthogneiss represents only a quarter of the crust. Orthogneiss melt fraction is often around 1 vol % at the metapelitic solidus when aqueous fluid exchange is considered, and can reach 4–5 vol % when orthogneiss represents a quarter of the crust. Depending on the fraction of metapelite and orthogneiss within the crust section considered, the amount of aqueous fluid transferred to orthogneiss varies and highly influences melt fraction predicted in orthogneiss (Fig. 4d).

Alternatively, under low-pressure conditions (<0.7 GPa), the muscovite dehydration reaction occurs at lower temperatures (∼680°C), generating large amounts of melt (>5 vol %) within the metapelite and limiting the importance of water-flux melting reactions.

Metagraywacke & orthogneiss

In the absence of aqueous fluid exchange (blue arrows, Fig. 4e), the model indicates that orthogneiss is often more fertile than metagraywacke for temperatures below 750°C (Fig. 4e). These relatively high melt fractions are related to muscovite-consuming reactions, which are more limited in the metagraywacke due to lower muscovite fractions.

Under mid-pressure conditions (∼0.7–1.2 GPa), orthogneiss becomes more fertile than metagraywacke when aqueous fluid transfer is activated. In these cases, the influx of external aqueous fluid can increase the orthogneiss melt fractions enough to make it the most fertile lithology up to 750°C (Fig. 4e). Since the predicted amount of aqueous fluid released by the metagraywacke is smaller than that released by metapelites, the effect of aqueous fluid exchange between the two lithologies is less significant. At the metagraywacke solidus, the orthogneiss melt fractions are mainly around 1 vol % (Fig. 4f), except few trajectories producing few percents due to muscovite dehydration occurring at low-*P* (trajectories 1 and 3).

Melt composition

The evolution of melt compositions as a function of temperature are shown in Ab–An–Or and Qz–Pl–Kfs ternary diagrams (Fig. 3g and h) and binary diagrams (supplementary files). These projections show that the melt compositions produced by the three lithologies are An-poor (Fig. 3g) and Qz-rich (Fig. 3h). However, melt compositions produced by metapelite and metagraywacke are Or/Kfs-depleted compared to those produced by orthogneiss and show a progressive Or/Kfs enrichment with increasing temperature (Fig. 3g and h). In contrast, melt compositions from orthogneiss vary less and instead show an increase in Ab/Pl contents, except for *P*–*T* trajectories with decreasing pressure, which show a slight decrease in Ab/Pl contents. The amount of aqueous fluid added to the orthogneiss system does not change the predicted melt compositions (see supplementary file). These differences reflect variations in Na_2O and K_2O contents (Table S2 and supplementary materials), which are related to the composition of the reactants: Kfs is richer in K_2O than Ms, and water-flux melting reactions in metasedimentary rocks are related to Pl breakdown, an Na_2O-rich phase. Therefore, the anatectic reaction in orthogneiss (Kfs + Pl + Qz + H_2O (+ Ms) → L) produces K_2O-enriched and Na_2O-depleted melts compared to the anatectic reaction in metapelite and metagraywacke (Ms + Pl + Qz + H_2O → L). All modelled melt compositions are consistent with experimental and natural data (Johannes & Holtz, 1996).

Discussion

Effects of *P*–*T* trajectory and fractionation on phase equilibrium predictions

Several studies have already demonstrated the effect of *P*–*T* path on mineral assemblages predicted by phase equilibrium models (de Capitani & Petrakakis, 2010; Yakymchuk & Brown, 2014; Yakymchuk *et al.,* 2017; Mayne *et al.,* 2016; Villaros *et al.,* 2018), as well as garnet fractionation (Lanari & Engi, 2017; Kendrick & Yakymchuk, 2020; Pan *et al.,* 2020). Integrating *P*–*T* trajectory-dependency into our model significantly affect the amounts of aqueous fluid produced by the metasedimentary rocks and the melt production in orthogneiss due to the distinct metamorphic reactions that occur along different *P–T* paths in the two lithologies.

The amount of aqueous fluid predicted to be released during the prograde paths is also influenced by the garnet fractionation (removal of garnet composition from reactive bulk composition, see section Methodology). Indeed, garnet fractionation decreases the amount of garnet formed along prograde trajectories (Lanari & Engi, 2017), thereby increasing the stability of hydrous minerals. For some trajectories under medium-pressure conditions, garnet fractionation also prevents the production of staurolite ($Ms + Grt \rightarrow Bt + St + Pl + Qz + H_2O$), which form later by the consumption of micas ($Pg + Bt + Qz \rightarrow St + Ms + Pl + H_2O$) also producing aqueous fluid. Therefore, the amount of aqueous fluid produced by garnet fractionation models is therefore considered as minimum values and would be higher if garnet re-equilibrated. The amount of garnet that crystallizes—and is therefore fractionated from the reactive part of the system—depends on the *P–T* trajectory. For example, the amount of garnet formed increases with pressure along the *P–T* trajectories (Lanari & Engi, 2017). Therefore, our study cannot be reproduced without defining *P–T* trajectory and it emphasizes the importance of path-definition in thermodynamic modelling. Nevertheless, a recent study by Tesser *et al.* (2025) has shown that garnet is partially dissolved in metapelite at the onset of partial melting, suggesting that its behavior is more complex than a simple refractory phase. Furthermore, garnet is not the only mineral that does not undergo continuous re-equilibration during prograde metamorphism and should be fractionated (e.g. plagioclase and muscovite; Lanari & Hermann, 2021). However, our current knowledge of the re-equilibration of metamorphic assemblages is limited and requires further investigations for inclusion in our models.

Melt fertility in the orogenic crust

Our results demonstrate that metasedimentary rocks can produce small quantities of aqueous fluid (<0.02 wt %) during prograde metamorphism, which can trigger water-flux partial melting in orthogneiss (Fig. 4). This small amount of aqueous fluid is enough to expand the *P–T* window in which orthogneiss is the most fertile lithology in the orogenic crust. It can also increase the melt fraction of orthogneiss by several percent (Fig. 4). A positive correlation is observed between the proportion of metasedimentary rocks in the model and the quantity of melt produced in the orthogneiss (Fig. 4c to f). Therefore, water-flux partial melting of metagranitoid rocks can be enhanced by aqueous fluid released by the surrounding metasedimentary rocks. Our results indicate that this process is particularly significant in metapelitic crust containing small bodies of orthogneiss, a common feature in orogenic crusts (*Variscan belt*: Martínez-Catalán *et al.*, 2021, *Pan-African belts*: Fritz *et al.*, 2013, *Himalayan belt*: Pognante, 1992; Finch *et al.*, 2014; Weinberg, 2016; Wang *et al.*, 2022). The results also emphasize that melt fractions in metagraywacke are so low at temperatures below 750°C that melt fractions in orthogneiss are always higher. Metabasites should also melt at higher temperature than orthogneisses (see solidi in Weinberg & Hasalová, 2015), and thus could contribute to its water-flux partial melting. Therefore, orthogneiss appears to be one of the most fertile lithology within heterogeneous orogenic crusts at temperatures below 750°C. These results demonstrate the potential of considering heterogeneous lithologies in modeled systems as soon as fluids or melts might migrate from one lithology to another (e.g. White *et al.*, 2005; Markmann & Lanari, 2026). On the other hand, our results also highlight that the aqueous fluid released by local metasedimentary rocks cannot produce large melt fractions in orthogneisses (>20 vol %), except if the fraction of orthogneisses is extremely small compared to metapelites (about 1/8). In addition, we used representative bulk compositions for each lithology, but it is highly probable that variations of these bulk compositions would influence solidus conditions and fertility of each lithology. Similarly, some accessories elements can lower solidus conditions (e.g. Li, B, or F; Johannes & Holtz, 1996), which would also affect the fertility of each lithology. Finally, melt compositions from metasedimentary rocks are richer in Na_2O and poorer in K_2O than the melt composition from orthogneiss (Fig. 3g and h), which could help to identify melt sources.

Implications for strain localization and tectonic evolution

The influx of external aqueous fluid produced by the metasedimentary rocks can generate several percent volume melt in orthogneiss, while the metasedimentary rocks are not yet molten or less fertile (Fig. 4c to f). Based on experimental data (Van der Molen & Paterson, 1979; Rutter & Neumann, 1995; Rushmer, 1995; Holyoke III & Rushmer, 2002; Rosenberg & Handy, 2005), it appears that the strength resistivity of metagranitoid lithologies decreases by ∼150 MPa for each percent of melt until reaching 7–8 vol %. Therefore, even if this process cannot produce significant amounts of melt in the orogenic crust, it can cause substantial reductions in the strength of metagranitic bodies, which may control strain localization in the orogenic crust. If the melt fraction in orthogneiss is higher than in metasedimentary rocks, deformation will be localized in the orthogneiss. As soon as metasedimentary rocks become more fertile, they will control ongoing strain localization. In addition, at subsolidus conditions during the prograde and retrograde path, strain localization is controlled by the amount of micas, grain size and inherited structures, often corresponding to metapelites (Hunter *et al.*, 2016). Therefore, along a prograde path reaching suprasolidus conditions, strain localization will be first controlled by metapelites, then by orthogneiss and finally by metapelites again.

Shear zones nucleated within metagranitoid rocks can act as preferential pathways for additional external water and/or melt influxes (Mogk, 1992; Mancktelow, 2006; Sawyer, 2010; Tafur & Diener, 2020; Etheridge *et al.*, 2021). These additional influxes of external aqueous fluid enhance partial melting via water-flux reaction in metagranitoid lithologies, increasing their melt fraction and decreasing their strength resistivity (Rosenberg & Handy, 2005). Thus, it can localize ongoing deformation and create a positive feedback loop. Therefore, we propose that the partial melting of metagranitoid rocks induced by the release of aqueous fluid from neighboring metasedimentary rocks initiates this positive feedback loop, inducing the strain localization within the metagranitic bodies during prograde metamorphism when reaching their solidus.

The transcurrent crustal-scale East Variscan Shear Zone passing through the Aiguilles-Rouges and Mont-Blanc massifs is an example of where this process has likely occurred. In this area, the suprasolidus anastomosed shear zones are located within the migmatitic orthogneisses and the surrounding metasedimentary rocks have reached lower melt fractions (Vanardois *et al.*, 2022, 2024). Field observations indicate that the partial melting of orthogneisses began with a planar fabric anterior to the first transcurrent shear zones, and subsequent transcurrent shear zones are localized within these molten orthogneisses. This indicates water-flux partial melting of the orthogneisses during prograde metamorphism controlled the strain localization and the formation of the shear zones. Then, evidence of additional hydrous melt injections and water-influxes promoting partial melting within the shear zones (Genier *et al.,* 2008; Vanardois *et al.,* 2022) illustrates the positive feedback loop described above. Our current study provides an explanation on the origin of aqueous fluid allowing the partial melting of the orthogneisses and their control and shear zones localization in the Aiguilles-Rouges and Mont-Blanc massifs.

Based on thermo-kinematic models simulating crustal thickening, *P–T* trajectories mainly reach the wet-solidus conditions during thermal relaxation and decompression (England & Thompson, 1984; Copley & Weller, 2022). Our results indicate that these trajectories are among the ones producing the most water in metasedimentary rocks and melt in orthogneiss (Fig. 4), suggesting that this process is likely to occur in continental collisions. Given the numerous occurrences of strain localization within water-flux partially molten metagranitoid rocks in ancient and recent orogens described around the world (Fig. 1), this process appears to be common during orogenic evolution and should be incorporated into future tectonic models.

Conclusion

We presented a path-dependent multi-lithological phase equilibrium model that emphasizes that the small amount of aqueous fluid released by metasedimentary rocks during prograde metamorphism is sufficient to enhance water-flux partial melting in orthogneiss. The results suggest that orthogneiss is commonly the most fertile lithology in heterogeneous orogenic crust at amphibolitic facies. Although melt fractions produced in orthogneiss are relatively small (<10 vol % for $T < 750°C$) for crust composed from 1/2 to 1/4 of orthogneiss, they can be sufficient to control strain localization in the middle and lower orogenic crust. It could allow for the nucleation of shear zones that would act as preferential pathways for additional aqueous fluid and melt influxes, which could create a positive feedback loop.

Supplementary data

Supplementary data are available at *Journal of Petrology* online.

Acknowledgements

We thank Noralinde de Leijer and Philip Hartmeier for constructive discussions. This work was supported by the European Research Council (ERC) under the European Union's Horizon 2020 research and innovation program (grant 850530) and from the Swiss National Science Foundation (grant 10007192). We thank Roberto Weinberg, Leo Kriegsman and an anonymous reviewer for constructive comments, and Jörg Hermann and Georg Zellmer for editorial handling.

Data availability

The Julia package WaterMeltPT.jl is available at https://github.com/jvanardo/Water-Melt-PT.jl and at https://doi.org/10.5281/zenodo.18337971.

References

Annen, C. & Sparks, R. S. J. (2002). Effects of repetitive emplacement of basaltic intrusions on thermal evolution and melt generation in the crust. *Earth and Planetary Science Letters* **203**(3–4), 937–955. https://doi.org/10.1016/S0012-821X(02)00929-9.

Berger, A., Burri, T., Alt-Epping, P. & Engi, M. (2008). Tectonically controlled fluid flow and water-assisted melting in the middle crust: an example from the Central Alps. *Lithos* **102**(3–4), 598–615. https://doi.org/10.1016/j.lithos.2007.07.027.

Brown, M. (2013). Granite: from genesis to emplacement. *GSA Bulletin* **125**(7–8), 1079–1113. https://doi.org/10.1130/B30877.1.

Burri, T., Berger, A. & Engi, M. (2005). Tertiary migmatites in the Central Alps: regional distribution, field relations, conditions of formation, and tectonic implications. *Schweizerische Mineralogische und Petrographische Mitteilungen* **85**(2–3), 215–232.

Carvalho, B. B., Sawyer, E. W. & Janasi, V. D. A. (2016). Crustal reworking in a shear zone: transformation of metagranite to migmatite. *Journal of Metamorphic Geology* **34**(3), 237–264. https://doi.org/10.1111/jmg.12180.

Clemens, J. D. (2012). Granitic magmatism, from source to emplacement: a personal view. *Applied Earth Science* **121**(3), 107–136. https://doi.org/10.1179/1743275813Y.0000000023.

Clemens, J. D. & Droop, G. T. R. (1998). Fluids, P–T paths and the fates of anatectic melts in the Earth's crust. *Lithos* **44**(1–2), 21–36. https://doi.org/10.1016/S0024-4937(98)00020-6.

Clemens, J. D. & Vielzeuf, D. (1987). Constraints on melting and magma production in the crust. *Earth and Planetary Science Letters* **86**(2–4), 287–306. https://doi.org/10.1016/0012-821X(87)90227-5.

Clemens, J. D., Stevens, G. & Bryan, S. E. (2020). Conditions during the formation of granitic magmas by crustal melting–hot or cold; drenched, damp or dry? *Earth-Science Reviews* **200**, 102982. https://doi.org/10.1016/j.earscirev.2019.102982.

Collins, W. J., Flood, R. H., Vernon, R. H. & Shaw, S. E. (1989). The Wuluma granite, Arunta block, Central Australia: an example of in situ, near-isochemical granite formation in a granulite-facies terrane. *Lithos* **23**(1–2), 63–83. https://doi.org/10.1016/0024-4937(89)90023-6.

Collins, W. J., Murphy, J. B., Johnson, T. E. & Huang, H. Q. (2020). Critical role of water in the formation of continental crust. *Nature Geoscience* **13**(5), 331–338. https://doi.org/10.1038/s41561-020-0573-6.

Copley, A. & Weller, O. (2022). The controls on the thermal evolution of continental mountain ranges. *Journal of Metamorphic Geology* **40**(7), 1235–1270. https://doi.org/10.1111/jmg.12664.

Couzinié, S., Bouilhol, P., Laurent, O., Marko, L. & Moyen, J. F. (2021). When zircon drowns: elusive geochronological record of water-fluxed orthogneiss melting in the Velay dome (massif central, France). *Lithos* **384-385**, 105938. https://doi.org/10.1016/j.lithos.2020.105938.

Davidson, J., Turner, S., Handley, H., Macpherson, C. & Dosseto, A. (2007). Amphibole "sponge" in arc crust? *Geology* **35**(9), 787–790. https://doi.org/10.1130/G23637A.1.

De Capitani, C. & Petrakakis, K. (2010). The computation of equilibrium assemblage diagrams with Theriak/domino software. *American Mineralogist* **95**(7), 1006–1016. https://doi.org/10.2138/am.2010.3354.

Delinardo-Silva, M. A., Monteiro, L. V. S., Moreto, C. P. N., Faustinoni, J., Santos, T. J. S., Sousa, S. D. & Xavier, R. P. (2025). From source to sink: U-Pb geochronology and Lithochemistry unraveling the missing link between Mesoarchean Anatexis and magmatism in the Carajás Province. *Brazil. Minerals* **15**(3), 265. https://doi.org/10.3390/min15030265.

Droop, G. T. R. & Brodie, K. H. (2012). Anatectic melt volumes in the thermal aureole of the Etive complex, Scotland: the roles of fluid-present and fluid-absent melting. *Journal of Metamorphic Geology* **30**(8), 843–864. https://doi.org/10.1111/j.1525-1314.2012.01001.x.

England, P. C. & Thompson, A. B. (1984). Pressure—temperature—time paths of regional metamorphism I. Heat transfer during the evolution of regions of thickened continental crust. *Journal of Petrology* **25**(4), 894–928. https://doi.org/10.1093/petrology/25.4.894.

Escuder Viruete, J. (1999). Hornblende-bearing leucosome development during syn-orogenic crustal extension in the Tormes gneiss dome, NW Iberian massif. *Spain. Lithos* **46**(4), 751–772. https://doi.org/10.1016/S0024-4937(99)00002-X.

Etheridge, M. A., Daczko, N. R., Chapman, T. & Stuart, C. A. (2021). Mechanisms of melt extraction during lower crustal partial melting. *Journal of Metamorphic Geology* **39**(1), 57–75. https://doi.org/10.1111/jmg.12561.

Ferreira, A. C., Dantas, E. L., Fuck, R. A., Nedel, I. M. & Reimold, W. U. (2021). Multiple stages of migmatite generation during the Archean to Proterozoic crustal evolution in the Borborema Province, Northeast Brazil. *Gondwana Research* **90**, 314–334. https://doi.org/10.1016/j.gr.2020.09.005.

Finch, M., Hasalová, P., Weinberg, R. F. & Fanning, C. M. (2014). Switch from thrusting to normal shearing in the Zanskar shear zone, NW Himalaya: implications for channel flow. *GSA Bulletin* **126**(7–8), 892–924. https://doi.org/10.1130/B30817.1.

Forshaw, J. B. & Pattison, D. R. (2023). Major-element geochemistry of pelites. *Geology* **51**(1), 39–43. https://doi.org/10.1130/G50542.1.

França, R. H., Neves, S. P., Bezerra, J. P. & Bruguier, O. (2019). Geochemistry and geochronology of orthogneisses across a major transcurrent shear zone (East Pernambuco shear zone, Borborema Province, Northeast Brazil): tectonic implications. *Journal of South American Earth Sciences* **91**, 285–301. https://doi.org/10.1016/j.jsames.2019.02.015.

Fritz, H., Abdelsalam, M., Ali, K. A., Bingen, B., Collins, A. S., Fowler, A. R., Ghebreab, W., Hauzenberger, C. A., Johnson, P. R., Kusky, T. M., Macey, P., Muhongo, S., Stern, R. J. & Viola, G. (2013). Orogen styles in the east African Orogen: a review of the Neoproterozoic to Cambrian tectonic evolution. *Journal of African Earth Sciences* **86**, 65–106. https://doi.org/10.1016/j.jafrearsci.2013.06.004.

García-Arias, M., Corretgé, L. G., Fernández, C. & Castro, A. (2015). Water-present melting in the middle crust: the case of the Ollo de Sapo gneiss in the Iberian massif (Spain). *Chemical Geology* **419**, 176–191. https://doi.org/10.1016/j.chemgeo.2015.10.040.

Gardien, V., Thompson, A. B. & Ulmer, P. (2000). Melting of biotite+ plagioclase+ quartz gneisses: the role of H2O in the stability of amphibole. *Journal of Petrology* **41**(5), 651–666. https://doi.org/10.1093/petrology/41.5.651.

Gardner, R., Piazolo, S., Evans, L. & Daczko, N. (2017). Patterns of strain localization in heterogeneous, polycrystalline rocks–a numerical perspective. *Earth and Planetary Science Letters* **463**, 253–265. https://doi.org/10.1016/j.epsl.2017.01.039.

Genier, F., Bussy, F., Epard, J. L. & Baumgartner, L. (2008). Water-assisted migmatization of metagraywackes in a Variscan shear zone, aiguilles-rouges massif, western Alps. *Lithos* **102**(3–4), 575–597. https://doi.org/10.1016/j.lithos.2007.07.024.

Hasalová, P., Štípská, P., Powell, R., Schulmann, K., Janoušek, V. & Lexa, O. (2008). Transforming mylonitic metagranite by open-system interactions during melt flow. *Journal of Metamorphic Geology* **26**(1), 55–80. https://doi.org/10.1111/j.1525-1314.2007.00744.x.

Holyoke, C. W., III & Rushmer, T. (2002). An experimental study of grain scale melt segregation mechanisms in two common crustal rock types. *Journal of Metamorphic Geology* **20**(5), 493–512. https://doi.org/10.1046/j.1525-1314.2002.00381.x.

Huang, W. L. & Wyllie, P. J. (1973). Melting relations of muscovite-granite to 35 kbar as a model for fusion of metamorphosed subducted oceanic sediments. *Contributions to Mineralogy and Petrology* **42**(1), 1–14. https://doi.org/10.1007/BF00521643.

Hunter, N. J., Hasalová, P., Weinberg, R. F. & Wilson, C. J. (2016). Fabric controls on strain accommodation in naturally deformed mylonites: the influence of interconnected micaceous layers. *Journal of Structural Geology* **83**, 180–193. https://doi.org/10.1016/j.jsg.2015.12.005.

Johannes, W. (1984). Beginning of melting in the granite system Qz-or-ab-an-H2O. *Contributions to Mineralogy and Petrology* **86**(3), 264–273. https://doi.org/10.1007/BF00373672.

Johannes, W. & Holtz, F. (1996) *Petrogenesis and Experimental Petrology of Granitic Rocks*. Berlin, Heidelberg: Springer-Verlag Berlin Heidelberg, p. 335.

Jung, C., Jung, S., Nebel, O., Hellebrand, E., Masberg, P. & Hoffer, E. (2009). Fluid-present melting of meta-igneous rocks and the generation of leucogranites—constraints from garnet major-and trace element data, Lu–Hf whole rock–garnet ages and whole rock Nd–Sr–Hf–O isotope data. *Lithos* **111**(3–4), 220–235. https://doi.org/10.1016/j.lithos.2008.11.008.

Kendrick, J. & Yakymchuk, C. (2020). Garnet fractionation, progressive melt loss and bulk composition variations in anatectic metabasites: complications for interpreting the geodynamic significance of TTGs. *Geoscience Frontiers* **11**(3), 745–763. https://doi.org/10.1016/j.gsf.2019.12.001.

Kumar, V., Honsberger, I. W., Kharya, A., Sachan, H. K., Rai, S. R. & Kumar, M. (2022). Mineralogical and fluid inclusion constraints on the formation of the Karakorum Migmatite: implications for H2O-fluxed melting and exhumation of the south Tibetan crust. *Contributions to Mineralogy and Petrology* **177**(6), 60. https://doi.org/10.1007/s00410-022-01927-4.

Lambert, C., Gervais, F., Crowley, J. L., Moukhsil, A. & Kavanagh-Lepage, C. (2023). Protracted melt-present deformation during the Rigolet phase of the Grenvillian orogeny. Insights from geochronology along the highway 117 transect through the Grenville Province in western Quebec, Canada. *Precambrian Research* **384**, 106939. https://doi.org/10.1016/j.precamres.2022.106939.

Lanari, P. & Engi, M. (2017). Local bulk composition effects on metamorphic mineral assemblages. *Reviews in Mineralogy and Geochemistry* **83**(1), 55–102. https://doi.org/10.2138/rmg.2017.83.3.

Lanari, P. & Hermann, J. (2021). Iterative thermodynamic modelling—part 2: tracing equilibrium relationships between minerals in metamorphic rocks. *Journal of Metamorphic Geology* **39**(6), 651–674. https://doi.org/10.1111/jmg.12575.

Lee, Y. & Cho, M. (2013). Fluid-present disequilibrium melting in Neoarchean arc-related migmatites of Daeijak Island, western Gyeonggi massif, Korea. *Lithos* **179**, 249–262. https://doi.org/10.1016/j.lithos.2013.08.011.

Lee, Y. & Cho, M. (2020). Fluid-present partial melting of Paleoproterozoic Okbang amphibolite in the Yeongnam massif. *Korea. Lithosphere* **2020**(1). https://doi.org/10.2113/2020/8854615.

Lee, Y., Cho, M. & Kim, J. (2023). Fluid-fluxed partial melting of the Buncheon granitic gneiss in the Yeongnam massif, Korea: protracted (ca. 1.86–1.84 Ga) reworking of the Paleoproterozoic Korean arc. *Lithos* **456**, 107308.

Levine, J. S. F. (2011) *In situ melt generation in anatectic migmatites and the role of strain in preferentially inducing melting*. PhD dissertation,. Austin: University of Texas.

Levy, D. A., Gordon, S. M., Zuza, A. V., Cisneros, M. & Kylander-Clark, A. R. (2025). Eocene-Oligocene metamorphism, fluid flow and deformation in the Ruby Mountains-East Humboldt range metamorphic core complex. *Tectonics* **44**(1), e2024TC008512. https://doi.org/10.1029/2024TC008512.

Li, Y., Sun, S., Dong, Y., He, D., Cheng, C., Yang, Z. & Zhang, B. (2023). Rheological behavior of amphibolite facies migmatites during orogenesis: a case study from the north Qinling Belt. *China. Lithos* **454-455**, 107240. https://doi.org/10.1016/j.lithos.2023.107240.

Liou, J. G., Tsujimori, T., Zhang, R. Y., Katayama, I. & Maruyama, S. (2004). Global UHP metamorphism and continental subduction/collision: the Himalayan model. *International Geology Review* **46**(1), 1–27. https://doi.org/10.2747/0020-6814.46.1.1.

Mancktelow, N. S. (2002). Finite-element modelling of shear zone development in viscoelastic materials and its implications for localisation of partial melting. *Journal of Structural Geology* **24**(6–7), 1045–1053. https://doi.org/10.1016/S0191-8141(01)00090-6.

Mancktelow, N. S. (2006). How ductile are ductile shear zones? *Geology* **34**(5), 345–348. https://doi.org/10.1130/G22260.1.

Markmann, T. A. & Lanari, P. (2026). Interplay between mechanical and petrochemical models on the fluid extraction from subduction zones. *Journal of Metamorphic Geology* **44**, 85–111. https://doi.org/10.1111/jmg.70015.

Martínez-Catalán, J. R., Schulmann, K. & Ghienne, J. F. (2021). The mid-Variscan allochthon: keys from correlation, partial retrodeformation and plate-tectonic reconstruction to unlock the geometry of a non-cylindrical belt. *Earth-Science Reviews* **220**, 103700. https://doi.org/10.1016/j.earscirev.2021.103700.

Mayne, M. J., Moyen, J. F., Stevens, G. & Kaislaniemi, L. (2016). Rcrust: a tool for calculating path-dependent open system processes and application to melt loss. *Journal of Metamorphic Geology* **34**(7), 663–682. https://doi.org/10.1111/jmg.12199.

Mintrone, M., Galli, A. & Schmidt, M. W. (2022). Exhumation of a migmatitic unit through self-enhanced magmatic weakening enabled by tectonic contact metamorphism (Gruf complex, central European Alps). *Contributions to Mineralogy and Petrology* **177**(5), 56. https://doi.org/10.1007/s00410-022-01919-4.

Mogk, D. W. (1992). Ductile shearing and migmatization at mid-crustal levels in an Archaean high-grade gneiss belt, northern Gallatin range, Montana, USA. *Journal of Metamorphic Geology* **10**(3), 427–438. https://doi.org/10.1111/j.1525-1314.1992.tb00094.x.

Pan, R., Macris, C. A. & Menold, C. A. (2020). Thermodynamic modeling of high-grade metabasites: a case study using the Tso Morari UHP eclogite. *Contributions to Mineralogy and Petrology* **175**(8), 78. https://doi.org/10.1007/s00410-020-01717-w.

Patiño Douce, A. E. & Harris, N. (1998). Experimental constraints on Himalayan anatexis. *Journal of Petrology* **39**(4), 689–710. https://doi.org/10.1093/petroj/39.4.689.

Piazolo, S., Daczko, N. R., Silva, D. & Raimondo, T. (2020). Melt-present shear zones enable intracontinental orogenesis. *Geology* **48**(7), 643–648. https://doi.org/10.1130/G47126.1.

Pognante, U. (1992). Migmatites and leucogranites of tertiary age from the high Himalayan Crystallines of Zanskar (NW India): a case history of anatexis of Palaeozoic orthogneisses. *Mineralogy and Petrology* **46**, 291–313. https://doi.org/10.1007/BF01173569.

Reichardt, H., Weinberg, R. F., Andersson, U. B. & Fanning, C. M. (2010). Hybridization of granitic magmas in the source: the origin of the Karakoram batholith, Ladakh. *NW India. Lithos* **116**(3–4), 249–272. https://doi.org/10.1016/j.lithos.2009.11.013.

Riel, N., Kaus, B. J., Green, E. C. R. & Berlie, N. (2022). MAGEMin, an efficient Gibbs energy minimizer: application to igneous systems. *Geochemistry, Geophysics, Geosystems* **23**(7), e2022GC010427. https://doi.org/10.1029/2022GC010427.

Rosenberg, C. L. & Handy, M. R. (2005). Experimental deformation of partially melted granite revisited: implications for the continental crust. *Journal of Metamorphic Geology* **23**(1), 19–28. https://doi.org/10.1111/j.1525-1314.2005.00555.x.

Rushmer, T. (1995). An experimental deformation study of partially molten amphibolite: application to low-melt fraction segregation. *Journal of Geophysical Research: Solid Earth* **100**(B8), 15681–15695. https://doi.org/10.1029/95JB00077.

Rutter, E. H. & Neumann, D. H. K. (1995). Experimental deformation of partially molten westerly granite under fluid-absent conditions, with implications for the extraction of granitic magmas. *Journal of Geophysical Research: Solid Earth* **100**(B8), 15697–15715. https://doi.org/10.1029/94JB03388.

Sawyer, E. W. (2010). Migmatites formed by water-fluxed partial melting of a leucogranodiorite protolith: microstructures in the residual rocks and source of the fluid. *Lithos* **116**(3–4), 273–286. https://doi.org/10.1016/j.lithos.2009.07.003.

Scalabrin, M., de Lima Muniz, R. & dos Santos, T. J. S. (2025). Zircon, monazite and titanite U-Pb geochronology revealing Orosirian metamorphic events within the Guiana shield. *Amazonian Craton. Precambrian Research* **422**, 107766. https://doi.org/10.1016/j.precamres.2025.107766.

Slagstad, T., Jamieson, R. A. & Culshaw, N. G. (2005). Formation, crystallization, and migration of melt in the mid-orogenic crust: Muskoka domain migmatites, Grenville Province. *Ontario. Journal of Petrology* **46**(5), 893–919. https://doi.org/10.1093/petrology/egi004.

Sperandio, D. G., Kuchenbecker, M., Barbuena, D. & Martini, A. (2025). Records of 2.9 Ga crustal anatexis on south American crust-source and melt segregation in the Porteirinha complex, Araçuaí Orogen (SE, Brazil). *Journal of South American Earth Sciences* **155**, 105418. https://doi.org/10.1016/j.jsames.2025.105418.

Tafur, L. A. & Diener, J. F. (2020). Mineral equilibrium constraints on the feasibility of diffusive H2O-fluxed melting in the continental crust. *Journal of Metamorphic Geology* **38**(7), 719–742. https://doi.org/10.1111/jmg.12536.

Tao, L., Cao, S., Li, W., Cheng, X., Liu, J., Dong, Y. *et al.* (2025). Water-fluxed melting and rheological weakening within the continental-scale Ailaoshan-Red River strike-slip shear zone, Western Yunnan. *China. Journal of Structural Geology* **197**, 105416. https://doi.org/10.1016/j.jsg.2025.105416.

Tesser, L. R., Lanari, P., Forshaw, J. B., Markmann, T. A., Hueck, M., Putlitz, B. *et al.* (2025). Melting the myth: prograde garnet dissolves during early crustal melting. *Geology*. .

Thompson, A. B. (1983). Fluid-absent metamorphism. *Journal of the Geological Society* **140**(4), 533–547. https://doi.org/10.1144/gsjgs.140.4.0533.

Van der Molen, I. & Paterson, M. S. (1979). Experimental deformation of partially-melted granite. *Contributions to Mineralogy and Petrology* **70**(3), 299–318. https://doi.org/10.1007/BF00375359.

Vanardois, J., Trap, P., Roger, F., Melleton, J., Marquer, D., Paquette, J. L., Goncalves, P., Cagnard, F. & Le Bayon, B. (2022). Deformation, crustal melting and magmatism in the crustal-scale east-Variscan shear zone (aiguilles-rouges and Mont-Blanc massifs, Western Alps). *Journal of Structural Geology* **163**, 104724. https://doi.org/10.1016/j.jsg.2022.104724.

Vanardois, J., Trap, P. & Marquer, D. (2024). Crucial role of water-present melting in metagranite: implications for the instigation of crustal-scale shear zones. *Geology* **52**(3), 199–204. https://doi.org/10.1130/G51790.1.

Vanderhaeghe, O. (2009). Migmatites, granites and orogeny: flow modes of partially-molten rocks and magmas associated with melt/solid segregation in orogenic belts. *Tectonophysics* **477**(3–4), 119–134. https://doi.org/10.1016/j.tecto.2009.06.021.

Varga, J., Raimondo, T., Hand, M., Curtis, S. & Daczko, N. (2022). Hydration, melt production and rheological weakening within an intracontinental gneiss dome. *Lithos* **432**, 106872.

Viegas, L. G. F., Archanjo, C. J., Hollanda, M. H. B. & Vauchez, A. (2014). Microfabrics and zircon U–Pb (SHRIMP) chronology of mylonites from the Patos shear zone (Borborema Province, NE Brazil). *Precambrian Research* **243**, 1–17. https://doi.org/10.1016/j.precamres.2013.12.020.

Vielzeuf, D. & Montel, J. M. (1994). Partial melting of metagreywackes. Part I. Fluid-absent experiments and phase relationships. *Contributions to Mineralogy and Petrology* **117**(4), 375–393. https://doi.org/10.1007/BF00307272.

Villaros, A., Laurent, O., Couzinié, S., Moyen, J. F. & Mintrone, M. (2018). Plutons and domes: the consequences of anatectic magma extraction—example from the southeastern French massif central. *International Journal of Earth Sciences* **107**(8), 2819–2842. https://doi.org/10.1007/s00531-018-1630-x.

Volante, S., Collins, W. J., Blereau, E., Pourteau, A., Spencer, C., Evans, N. J. *et al.* (2020). Reassessing zircon-monazite thermometry with thermodynamic modelling: insights from the Georgetown igneous complex, NE Australia. *Contributions to Mineralogy and Petrology* **175**(12), 110. https://doi.org/10.1007/s00410-020-01752-7.

Volante, S., Pourteau, A., Li, Z. X., Collins, W. J., Doucet, L. S., Olierook, H. K., Martin, L. & Smit, M. A. (2025). Oxygen isotope shifts reveal fluid-fluxed melting in continental anatexis. *Communications Earth & Environment* **6**(1), 282. https://doi.org/10.1038/s43247-025-02250-z.

Wang, J., Wu, F., Zhang, J., Khanal, G. & Yang, L. (2022). The Himalayan collisional orogeny: a metamorphic perspective. *Acta Geologica Sinica-English Edition* **96**(6), 1842–1866. https://doi.org/10.1111/1755-6724.15022.

Warr, L. N. (2021). IMA–CNMNC approved mineral symbols. *Mineralogical Magazine* **85**(3), 291–320. https://doi.org/10.1180/mgm.2021.43.

Webb, G., Powell, R. T. J. B. & McLaren, S. (2015). Phase equilibria constraints on the melt fertility of crustal rocks: the effect of subsolidus water loss. *Journal of Metamorphic Geology* **33**(2), 147–165. https://doi.org/10.1111/jmg.12114.

Weinberg, R. F. (2016). Himalayan leucogranites and migmatites: nature, timing and duration of anatexis. *Journal of Metamorphic Geology* **34**(8), 821–843. https://doi.org/10.1111/jmg.12204.

Weinberg, R. F. & Hasalová, P. (2015). Water-fluxed melting of the continental crust: a review. *Lithos* **212-215**, 158–188. https://doi.org/10.1016/j.lithos.2014.08.021.

Weisbrod, A. (1970) *Petrology of the metamorphic socle of the central Cevennes (French Massif central). Sedimentalogical reconstruction and thermodynamic approach of metamorphism*. PhD dissertation,. Nancy: Université de Nancy.

White, R. W., Pomroy, N. E. & Powell, R. (2005). An in situ metatexite–diatexite transition in upper amphibolite facies rocks from Broken Hill. *Australia. Journal of Metamorphic Geology* **23**(7), 579–602. https://doi.org/10.1111/j.1525-1314.2005.00597.x.

White, R. W., Powell, R., Holland, T. J. B., Johnson, T. E. & Green, E. C. R. (2014). New mineral activity–composition relations for thermodynamic calculations in metapelitic systems. *Journal of Metamorphic Geology* **32**(3), 261–286. https://doi.org/10.1111/jmg.12071.

Winkler, H. G. & Von Platen, H. (1958). Experimentelle gesteinsmetamorphose—II: Bildung von anatektischen granitischen schmelzen bei der metamorphose von NaCl-führenden kalkfreien Tonen. *Geochimica et Cosmochimica Acta* **15**(1–2), 91–112.

Winkler, H. G. F. & Von Platen, H. (1960). Experimentelle gesteinsmetamorphose—III: Anatektische ultrametamorphose kalkhaltiger tone. *Geochimica et Cosmochimica Acta* **18**(3–4), 294–316. https://doi.org/10.1016/0016-7037(60)90094-6.

Winkler, H. G. & von Platen, H. (1961). Experimentelle Gesteinsmetamorphose—IV: bildung anatektischer Schmelzen aus metamorphisierten Grauwacken. *Geochimica et Cosmochimica Acta* **24**(1–2), 48–69. https://doi.org/10.1016/0016-7037(61)90007-2.

Yakymchuk, C. & Brown, M. (2014). Consequences of open-system melting in tectonics. *Journal of the Geological Society* **171**(1), 21–40. https://doi.org/10.1144/jgs2013-039.

Yakymchuk, C., Clark, C. & White, R. W. (2017). Phase relations, reaction sequences and petrochronology. *Reviews in Mineralogy and Geochemistry* **83**(1), 13–53. https://doi.org/10.2138/rmg.2017.83.2.

Yardley, B. (2009). The role of water in the evolution of the continental crust. *Journal of the Geological Society* **166**(4), 585–600. https://doi.org/10.1144/0016-76492008-101.

Yardley, B. (2012). The permeability of crustal rocks through the metamorphic cycle: an overview. *Crustal permeability* , 275–284. https://doi.org/10.1002/9781119166573.ch22.

Journal of Petrology, 2026, 67(7),
https://doi.org/10.1093/petrology/egag052
Letter